Quaternary Research 76 (2011) 10–21

Contents lists available at ScienceDirect

Quaternary Research

journal homepage: www.elsevier.com/locate/yqres

Holocene eolian activation as a proxy for broad-scale landscape change on the Gila River Indian Community, Arizona

David K. Wright [a,b,*], Steven L. Forman [c], Michael R. Waters [d,e], John C. Ravesloot [f]

[a] Department of Archaeology and Art History, College of Humanities 14-201, Seoul National University, San 56-1, Sillim-9dong, Gwanak-gu, Seoul 151-745, Republic of Korea
[b] Cultural Resource Management Program, Gila River Indian Community, P.O. Box 2140, Sacaton, AZ 85247, USA
[c] Department of Earth and Environmental Sciences, University of Illinois at Chicago, Chicago, IL 60607, USA
[d] Center for the Study of the First Americans, Department of Anthropology,Texas A&M University, College Station, TX 77843, USA
[e] Department of Geography, Texas A&M University, College Station, TX 77843, USA
[f] William Self Associates, Inc., Tucson, AZ 85719, USA

ARTICLE INFO

Article history:
Received 14 July 2010
Available online 26 May 2011

Keywords:
Arizona
Gila River
Holocene
eolian activation
paleoclimates

ABSTRACT

Eolian sediments are common within the middle Gila River Valley, southern Arizona, and reflect variability in eolian and fluvial processes during the late Holocene. This study focuses on deciphering the stratigraphic record of eolian deposition and associated luminescence dating of quartz extracts by single aliquot regeneration (SAR) protocols. Stratigraphic assessment coupled with luminescence ages indicates that there are four broad eolian depositional events at ca. 3145 ± 220 yr, 1950–1360 yr, 800 ± 100 yr, and 690–315 yr. This nascent chronology, correlated with regional archeological evidence and paleoclimate proxy datasets, leads to two general conclusions: (1) loess deposits, transverse-dune formation and sand-sheet deposition in the late Holocene are probably linked to flow variability of the Gila River, though the last two events are concordant with regional megadroughts; and (2) the stability of eolian landforms since the 19th century reflects the lack of eolian sediment supply during a period of fluvial incision, resulting in Entisol formation on dunes. The prime catalyst of eolian activity during the late Holocene is inferred to be sediment supply, driven by climate periodicity and variable flow within the Gila River catchment.

Introduction

Southern Arizona currently has one of the largest population centers in the United States and includes large swaths of agricultural land irrigated with diverted water from the Colorado River. The region also hosted Pre-Columbian communities who made use of perennially flowing streams and rivers draining the surrounding uplands to maintain large tracts of cultivated plots (Haury, 1976; Bayman, 2001; Fish and Fish, 2008; Ravesloot et al., 2009). The present study area is situated within the Sonoran Desert, which is characterized by low rainfall (<25 cm/yr) and July temperatures that average 41°C. These circumstances make the study area particularly vulnerable to catastrophic droughts, which can devastate local economies and threaten livelihoods of the region's inhabitants. Understanding the geomorphic and climatic controls on broad-scale landscape change is important for potentially mitigating the effects of extreme oscillations in precarious environments such as southern Arizona.

Backhoe trenches excavated in 2005 and 2006 on landforms adjacent to the middle Gila River were analyzed for evidence of late Holocene eolian activity. The study area is located within the Gila River Indian Community (GRIC) and was undertaken with sponsorship of the Cultural Resource Management Program (CRMP) and the Pima–Maricopa Irrigation Project (P-MIP). The research objectives were designed to assess archeological site formation processes within eolian depositional areas, which are extensive across the GRIC. A series of optically stimulated luminescence (OSL) and radiocarbon (^{14}C) ages were generated to reveal local patterns of sand-sheet accretion and dune movement.

The studies performed included geomorphic and stratigraphic analysis of eolian and alluvial landforms. Specifically, we studied four trench exposures of eolian deposits, determined Optically Stimulated Luminescence (OSL) ages on quartz extracts from eolian sediments, and radiocarbon assays of cultural features at archeological site GR-893 that underlie the eolian deposits. The time series of eolian activity is compared to drought (http://www.ncdc.noaa.gov/paleo/paleo.html), river flow (Graybill et al., 2006) and fluvial geomorphic events (Waters and Ravesloot, 2001) to infer the most likely drivers of eolian deposition in the past 2000 years.

Eolian activity as a proxy for landscape change

The movement of sediments by wind necessitates three primary conditions: the availability of sediment suitably sized for entrainment

* Corresponding author at: Department of Archaeology and Art History, College of Humanities 14-201, Seoul National University, San 56-1, Sillim-9dong, Gwanak-gu, Seoul 151-745, Republic of Korea.
E-mail addresses: msafiri@snu.ac.kr (D.K. Wright), slf@uic.edu (S.L. Forman),

0033-5894/$ – see front matter © 2011 University of Washington. Published by Elsevier Inc. All rights reserved.
doi:10.1016/j.yqres.2011.04.008

by wind, a lack of stabilizing vegetation, and a wind velocity that exceeds the threshold needed for sediment transport (Pye and Tsoar, 1990:127–145). Sediment availability and supply typically originates from alluvial or colluvial settings whereby silts and fine sands move to channel margins where they are subsequently entrained in wind (Pye, 1995; Muhs et al., 2003). Eolian transport of silts (0.002–0.05 mm) and fine sands (0.05–0.25 mm) is a function of kinetic energy associated with wind shear specific to the grain size subject to entrainment (Anderson and Haff, 1988; Williams et al., 1993; Goossens and Offer, 1997; Butterfield, 1998). In the published models of eolian sediment transport, wind shear velocity (V) and stress (τ) for entrainment of silt grains is high and tapers to the lowest threshold for 0.1-mm diameter sand grains, then increases linearly for larger grains (e.g., Bagnold, 1941; Anderson and Hallet, 1986; Sarre, 1987; Shao, 2000).

In the deserts of the American Southwest during the Holocene, the inferred primary driver of eolian sand depositional systems is sediment supply, particularly from fluvial systems (Lancaster and Tchakerian, 2003). Multiproxy correlations among playa basin filling, fluvial system flow and dune aggradation in southeastern California through the late Quaternary appear stochastic, suggesting that aridity was not the prime driver of dune accretion (Kocurek and Lancaster, 1999; Tchakerian and Lancaster, 2002). Instead, individual events such as a high-magnitude storm or lateral channel migration provide sediment supply for dune formation or deflation events on sub-decadal time scale, which are difficult to detect in the paleoenvironmental record (Lancaster, 1997; Clarke and Rendell, 1998; Reheis et al., 2005). Other studies indicate that xerophytic vegetation acts as a sediment trap for eolian silts and sands and therefore dune accretion can be most prominent during pluvial phases, in which desert shrubs are abundant on dune slopes (Fearnehough et al., 1998).

Climate variability recorded in tree ring records over the past 2000 years, particularly associated with a succession of pluvial and extreme drought events, has provided a geomorphic context for landform destabilization and sediment entrainment by wind. Tree-ring time series from the southwestern United States indicate prehistoric droughts that surpassed conditions during the driest years in the 20th century (Cook et al., 2007; Stahle et al., 2007). In the southwestern United States, there are number of "megadroughts" that occur in the 13th, 14th and 16th centuries AD (Stahle et al., 2007) and other severe droughts in the 18th and 19th centuries AD (Woodhouse et al., 2002; Cook et al., 2007; Herweijer et al., 2007; Stahle et al., 2007). Significant and prolonged drying in the western United States is also associated with the Medieval Warm Period (ca. AD 800–1300). In turn, there were noticeable intervening wet (pluvial) periods (Woodhouse et al., 2005). Reactivation of eolian sand systems with periodic drought have been inferred in inter-mountain basins in southwestern Colorado with elongation of parabolic dunes ca. 1290–940, 715 ± 80, 320 ± 30, 200–100, and 1955 ± 10 yr (Forman et al., 2006).

Loess deposits are generally associated with regional- or global-scale climatic driving events (Smalley, 1966; Porter, 2001; Bettis et al., 2003). The sediment sources for glacial loess are found on outwash plains or exposed fluvial beds and are transported aloft via strong winds (Smalley, 1995; Kohfeld and Harrison, 2003; Muhs and Bettis, 2003). Loess is not widespread in desert environments but is more commonly distributed in the semiarid fringes of true deserts (Smalley and Vita-Finzi, 1968). The loess found in non-glacial contexts is derived from a variety of processes combined with fluvial sorting or eolian deflation plus ample wind speed sufficient for airborne sediment suspension (Smalley and Vita-Finzi, 1968; Wright, 2001). Accumulation of desert loess normally occurs in vegetation sediment traps or hollows on the landscape (Tsoar and Pye, 1987).

Geomorphic and climatic setting

The middle Gila River Valley is situated within the Sonoran Desert in the Basin and Range Province, and is locally referred to as the Phoenix Basin (Fig. 1). The climate of the region is characterized as hot and arid (Sellars and Hill, 1974). The mean annual temperature is 20.6°C, with July maximum temperatures averaging 41°C and January minimum temperatures averaging 1°C (Camp, 1986). The Phoenix Basin typically receives <250 mm/yr of precipitation, whereas portions of the Gila River headwaters fall within the 500–750 mm/yr isohyet (Sheppard et al., 2002). There is a slight moisture gradient that increases from west to east, and mean annual rainfall ranges from 19 cm at Maricopa to 21 cm at Sacaton to 24 cm at Florence (Sellars and Hill, 1974). The wettest months are typically July and August, during which afternoon thunderstorms develop and produce heavy but localized rainfall. A secondary period of precipitation occurs in the winter when large storms from the Pacific Ocean enter the region. Rainfall associated with these storms is typically gentle and widespread. The months of April, May, and June are the driest. Occasionally, late summer or early fall tropical storms from the eastern mid-Pacific are steered over Arizona and may contribute considerable rainfall to the region (Hirschboek, 1985; Smith, 1986). Local flooding outside the Gila River channel is typically sheetwash because the valley floor is very flat and topographically featureless.

Generally, the middle Gila River Valley is a water-deficient region, with potential evapotranspiration almost always exceeding precipitation (Waters, 1998). Analysis of a 1186-yr dendrochronology suggest that 20th-century estimates of average rainfall in the region are significantly higher than the long-term mean (Woodhouse et al., 2005). However, the region is extremely sensitive to variability in the El Niño–Southern Oscillation (ENSO) and Pacific Decadal Oscillation (PDO), resulting in significant interannual variability of precipitation (Sheppard et al., 2002). Surficial processes within the Gila River catchment were affected by decadal-scale periodicity of ENSO (Moy et al., 2002) and PDO (Biondi et al., 2001) during the middle to late Holocene (see also Bacon et al., 2010). Anthropogenic landscape modifications since the middle to late 19th century have desiccated the middle Gila River from its historic high flows, reducing it to an intermittent stream with no- or low-water flow for the majority of the year (Waters and Ravesloot, 2000; Eiselt et al., 2002; Darling et al., 2004:286).

Huckleberry (1993, 1994, 1995), Waters (2008) and Waters and Ravesloot (2000, 2001, 2003) present an evolutionary model of the middle Gila River showing a succession of channel aggradation events and downcutting events from the early Holocene that have incised and accreted on the Pleistocene substrate. Alluvial terraces are separated into four primary geomorphic units (T-0, T-1, T-2, T-3) based on the broad timeframes of accretion and subsequent changes in channel morphology that resulted in terrace incision ranging from 0.5 to 2 m deep (Waters, 1996; Waters and Ravesloot, 2000). The present project areas are situated on the adjacent eolian sand sheets (*Hess*) and dunes (*Hed*) that rest unconformably atop alluvial deposits. The *Hed* deposits are typically comprised of sparsely vegetated transverse dunes (Fig. 2).

A significant source of eolian particles within the GRIC originates from the channel of the middle Gila River. This river has aggraded and degraded numerous times in the past 2000 years (Waters and Ravesloot, 2000), providing a ready supply of sediment for eolian entrainment. These particles were moved primarily by winds from south to southwest based on the orientation of transverse dunes north of the Gila River, while sand sheets south and west of the Gila River accrete as a result of easterlies. Observed and averaged wind speeds and directions taken from the weather stations across the Phoenix metropolitan area from 1930 to 1996 indicates that prevailing wind directions are easterlies for all months except September, October, November, and December, where they average as westerlies (National Climatic Data Center, 1998).

OSL dating

OSL dating is based on the time-dependent dosimetric properties of silicate minerals, predominately quartz (Aitken, 1998). The advent

https://doi.org/10.1016/j.yqres.2011.04.008 Published online by Cambridge University Press

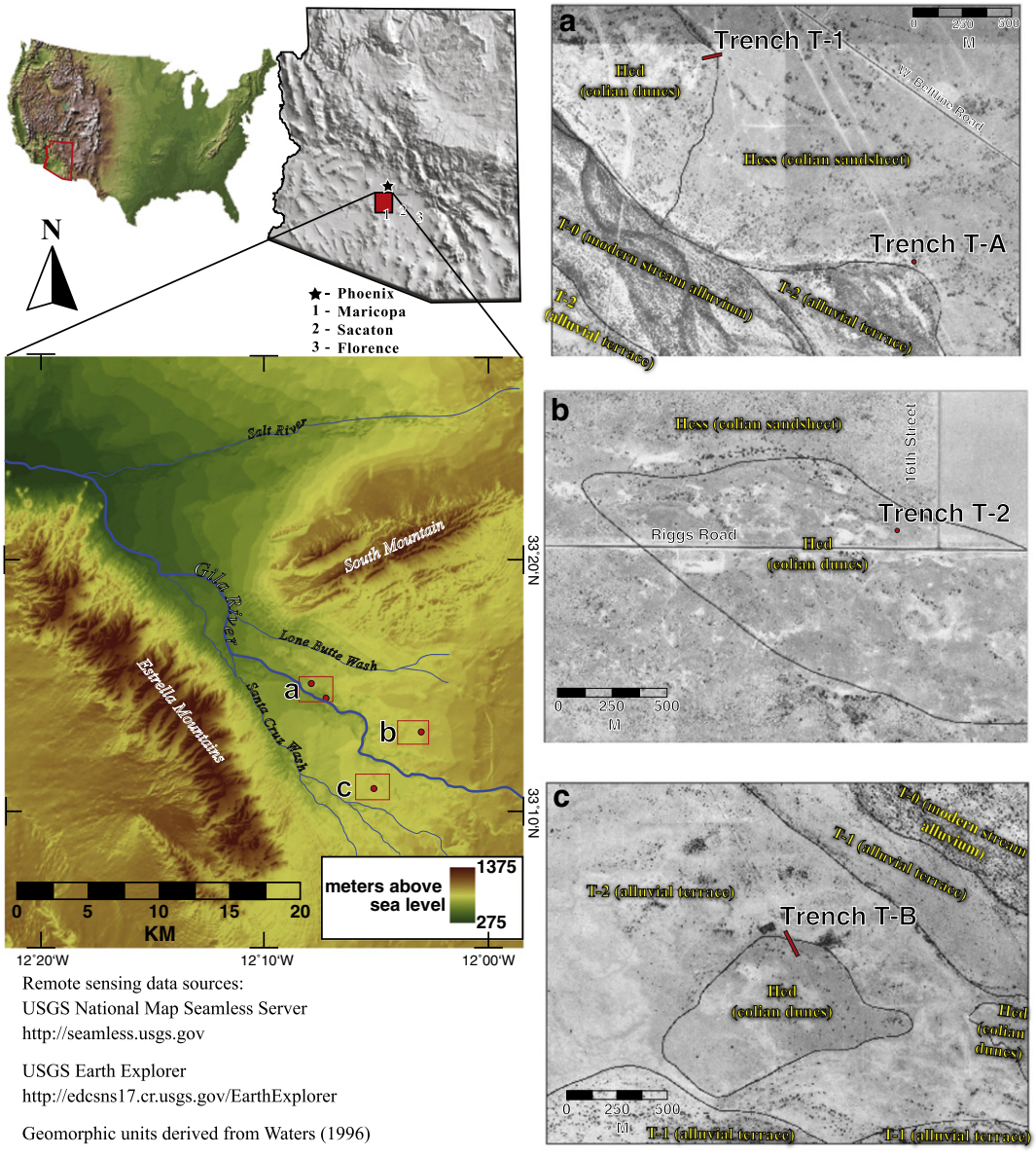

Figure 1. Location of the project area.

of single aliquot regeneration (SAR) protocols (e.g., Murray and Wintle, 2003; Wintle and Murray, 2006) for dating quartz grains provides improved accuracy and precision to yield new insight on the temporal and spatial patterns of eolian activity (e.g., Bailey et al., 2001; Murray and Clemmensen, 2001; Ballarini et al., 2003; Forman and Pierson, 2003; Stokes et al., 2004; Clemmensen and Murray, 2006).

In this study, medium-to-fine eolian sand associated with primary dune bedforms or sand-sheet deposits was sampled for OSL dating. SAR protocols (Murray and Wintle, 2003) were used in this study to estimate the equivalent dose of the 100–150 μm or 150–250 μm quartz fraction and, for one sample (UIC1548), the 4–11 μm quartz fraction (hydroflurosilicic acid digestion) for up to 45 separate aliquots (Table 1). Each aliquot covers 1 cm^2 on an aluminum disk and contains ~2000 to 5000 quartz grains. The sand-sized quartz fraction was isolated by density separations using the heavy liquid Na–polytungstate. A 40-minute immersion in 40% hydrofluoric acid (HF) was applied to dissolve non-quartz minerals and etch the outer 10+ microns of quartz grains, which are affected by alpha (α) radiation (Mejdahl and Christiansen, 1994). The purity of quartz separates was evaluated by petrographic inspection and point counting of a representative aliquot. Samples that showed >1% of non-quartz minerals were retreated with HF and rechecked petrographically. The purity of quartz separates was tested by exposing aliquots to infrared excitation (880 nm), which preferentially excites feldspar minerals. Samples measured showed weak emissions (<300 counts/s) at or close to background counts with infrared excitation, and ratios of emissions from blue to infrared excitation of >20, indicating a spectrally pure quartz extract (Duller et al., 2003).

An Automated Risø TL/OSL-DA-15 system (Bøtter-Jensen et al., 2000) was used for SAR analyses. Blue light excitation (470 ± 20 nm) was generated from an array of 30 light-emitting diodes that deliver ~15 mW/cm^2 to the sample position at 90% power. A Thorn EMI 9235 QA photomultiplier tube coupled with three 3-mm-thick Hoya U-340 detection filters, transmitting between 290 and 370 nm, measured photon emissions. Laboratory irradiations used a calibrated $^{90}Sr/^{90}Y$ beta source coupled with the Risø reader. All SAR emissions were integrated over the first 0.8 s of stimulation out of 50 s of measurement, with background based on emissions for the last 50- to 40-second interval.

https://doi.org/10.1016/j.yqres.2011.04.008 Published online by Cambridge University Press

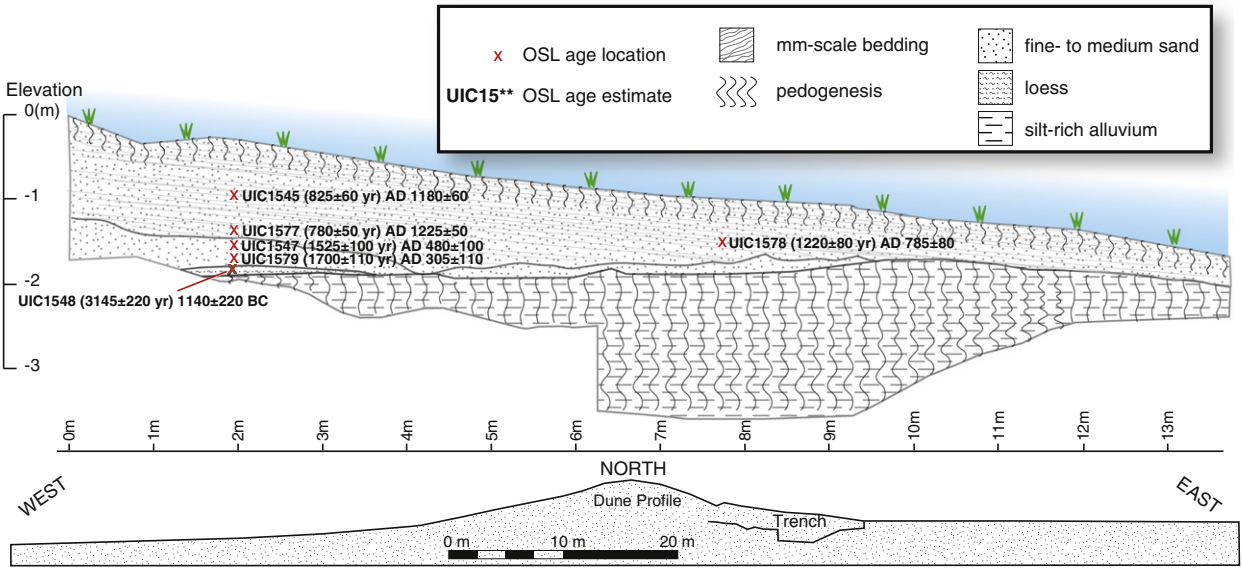

Figure 2. Stratigraphic profile of Trench T-1 with locations of age assays.

A series of experiments was performed to evaluate the effect of preheating at 180°, 200°, 220°, and 240°C on thermal transfer of the regenerative signal prior to the application of SAR dating protocols (Murray and Wintle, 2003). These experiments showed no preheat-based sensitivity changes and the samples were preheated to 220°C. Tests for dose reproducibility were also performed and the results showed the last dose coincided well with the initial dose (at one-sigma errors). Only aliquots with recycling ratios between 0.9 and 1.1 were retained in age calculations, which was for most samples all of the generated data.

A critical analysis for luminescence dating is the dose rate, which is an estimate of the exposure of the sediment to ionizing radiation from U and Th decay series, ^{40}K, and cosmic sources during the burial period (Table 1). The U and Th content of the dose rate samples, assuming secular equilibrium in the decay series and ^{40}K, were determined by inductively coupled plasma-mass spectrometry (ICP-MS) analyzed by Activation Laboratory Ltd., Ontario, Canada. The beta and gamma doses were adjusted according to grain diameter to compensate for mass attenuation (Fain et al., 1999). A small cosmic ray component between 0.21 and 0.17 ± 0.02 mGy/yr, depending on depth at which the sediment was buried, was included in the estimated dose rate (Prescott and Hutton, 1994). The moisture content (by weight) of 5 ± 2% to 10 ± 3% was assumed depending

Table 1
Single aliquot regeneration (SAR) ages on eolian sediments from the Gila River Indian Community, Arizona.

Sample number	Laboratory number	Fraction (μm)	Aliquots	Equivalent dose (Gray)[a]	U (ppm)[b]	Th (ppm)[b]	K_20 (%)[b]	Cosmic dose (mGray/yr)[c]	Moisture content (%)	Dose rate (mGray/yr)	Over-dispersion (%)	SAR age (yr)[d]
Dune T-1 (2005)												
94-14-T26-2	UIC1579	150–250	30	8.74 ± 0.34	6.1 ± 0.1	16.2 ± 0.1	2.73 ± 0.03	0.18 ± 0.02	5 ± 2	5.15 ± 0.22	14.7 ± 1.9	1700 ± 110
94-14-T26-4	UIC1547	100–150	30	5.68 ± 0.16	1.9 ± 0.1	6.2 ± 0.1	2.94 ± 0.03	0.19 ± 0.02	5 ± 2	3.74 ± 0.17	8.0 ± 1.0	1525 ± 100
94-14-T26-5	UIC1577	150–250	27	3.84 ± 0.14	4.4 ± 0.1	15.0 ± 0.1	3.01 ± 0.03	0.20 ± 0.02	5 ± 2	4.95 ± 0.20	9.2 ± 1.2	780 ± 50
94-14-T26-6	UIC1545	100–150	30	3.01 ± 0.10	1.5 ± 0.1	5.6 ± 0.1	2.98 ± 0.03	0.20 ± 0.02	5 ± 2	3.65 ± 0.17	16.5 ± 2.1	825 ± 60
94-14-726-9	UIC1578	150–250	30	5.52 ± 0.16	4.0 ± 0.1	16.6 ± 0.1	2.82 ± 0.03	0.19 ± 0.02	10 ± 3	4.52 ± 0.20	16.1 ± 2.1	1220 ± 80
94-14-T26-1	UIC1548	4–11	28	14.05 ± 0.38	2.2 ± 0.1	7.8 ± 0.1	2.87 ± 0.03	0.17 ± 0.01	10 ± 3	4.47 ± 0.20	13.9 ± 2.4	3145 ± 220
Dune T-2 (2005)												
94-14-T26-10	UIC1549	100–150	45	7.19 ± 0.25	2.0 ± 0.1	6.4 ± 0.1	3.05 ± 0.03	0.20 ± 0.02	5 ± 2	3.81 ± 0.17	16.0 ± 2.2	1885 ± 140
94-14-T26-11	UIC1546	100–150	30	5.26 ± 0.25	1.8 ± 0.1	6.6 ± 0.1	3.07 ± 0.03	0.21 ± 0.02	5 ± 2	3.87 ± 0.17	15.7 ± 2.0	1360 ± 110
Dune T-A (2006)												
GR1442-T3-6	UIC1759	150–250	30	7.62 ± 0.37	1.8 ± 0.1	7.4 ± 0.1	3.06 ± 0.03	0.18 ± 0.02	5 ± 2	3.83 ± 0.17	26.5 ± 3.4	1990 ± 185
GR1442-T3-7	UIC1754	100–150	30	7.30 ± 0.25	1.6 ± 0.1	6.3 ± 0.1	3.01 ± 0.03	0.19 ± 0.02	5 ± 2	3.74 ± 0.17	18.5 ± 2.4	1950 ± 150
Dune T-B (2006)												
GR893-96-1	UIC1758	150–250	30	2.02 ± 0.06	1.9 ± 0.1	7.9 ± 0.1	3.48 ± 0.03	0.20 ± 0.02	5 ± 2	4.28 ± 0.19	9.3 ± 1.2	470 ± 35
GR893-96-2	UIC1757	150–250	30	1.29 ± 0.04	1.7 ± 0.1	8.3 ± 0.1	3.33 ± 0.03	0.20 ± 0.02	5 ± 2	4.13 ± 0.18	17.4 ± 1.9	315 ± 20
GR893-96-2	UIC1757B[e]	150–250	30	1.33 ± 0.04	1.7 ± 0.1	8.3 ± 0.1	3.33 ± 0.03	0.20 ± 0.02	5 ± 2	4.13 ± 0.18	16.6 ± 2.1	325 ± 25
GR893-62-3	UIC1760	150–250	30	2.92 ± 0.10	1.9 ± 0.1	8.3 ± 0.1	3.41 ± 0.03	0.20 ± 0.02	5 ± 2	4.24 ± 0.19	14.2 ± 1.8	690 ± 50
GR893-62-4	UIC1756	150–250	30	2.17 ± 0.05	1.7 ± 0.1	7.7 ± 0.1	3.50 ± 0.04	0.21 ± 0.02	5 ± 2	4.24 ± 0.19	11.3 ± 1.5	510 ± 50
GR893-25-5	UIC1755	150–250	30	2.86 ± 0.10	2.0 ± 0.1	8.1 ± 0.1	3.42 ± 0.03	0.20 ± 0.02	5 ± 2	4.30 ± 0.19	4.8 ± 0.6	665 ± 50

[a] Quartz grains analyzed under blue-light excitation (470 ± 20 nm) by single aliquot regeneration protocols of Murray and Wintle (2003). The central age model of Galbraith et al. (1999) was used in equivalent dose calculations.
[b] U, Th and K_20 content analyzed by inductively coupled plasma-mass spectrometry analyzed by Activation Laboratory LTD, Ontario, Canada.
[c] From Prescott and Hutton (1994).
[d] All errors are at one sigma ages and are calculated from AD 2005. Analyses by Luminescence Dating Research Laboratory, Dept. of Earth and Environmental Sciences, University of Illinois at Chicago.
[e] Analyzed with initial infrared exposure (840 ± 40 nm) prior to blue light excitation.

https://doi.org/10.1016/j.yqres.2011.04.008 Published online by Cambridge University Press

on current conditions and stratigraphic association with aquitards, particularly buried soils. A sediment sample of analogous fraction to those being analyzed was collected, immediately weighed, stored in a low-humidity environment, and successively weighed over a period of 14 days. When the weight change was <0.25% in 1 day, the sample was assumed to be completely dry, and the estimate was made from the net change in weight. A central age model developed by Galbraith et al. (1999) was used to assume a log-normal distribution of equivalent dose values and corrects for data over-dispersion for age calculation. The errors associated with SAR dating are usually <5% yielding an error in calculated age of 6 to 8%. Optical ages are reported in years prior to AD 2005 (Table 1). In this manuscript, we have also included Gregorian calendar ages in order to have consistency between the calibrated radiocarbon calendar (which reports yr BP prior to AD 1950) and archeological chronologies from the American Southwest, which use the Gregorian calendar. To assess periods of eolian deposition and to facilitate intercomparison with previous studies optical ages are analyzed as a probability density function (Singhvi et al., 2001), with each peak reflecting the highest probability for an eolian depositional event.

Eolian stratigraphy and geochronology

Four trenches were excavated into dune and sand sheet deposits adjacent to the middle Gila River (Waters, 2005; Ravesloot et al., 2007; Wright and Forman, 2010). Eolian sediments and soils were assigned unit and soil designations based on sediment structure and morphology. Eolian depositional units documented in the four trenches are correlated based on bounding soils and OSL ages. In each trench, either a representative section of the exposure was described or, if an important contact was found, the entire profile was recorded. The thickness, depth, and sequence of sediments and soils were recorded. Sediment samples were collected for generating OSL age estimates. By recording and dating the eolian stratigraphy of landforms, the research design focused on understanding the onset and duration of eolian events within the middle Gila River floodplain and potential impacts of sediment accretion on archeological site taphonomy.

Trench T-1 was excavated in a stabilized transverse dune approximately 1 km from the modern channel of the Gila River and exposed three eolian depositional units spanning the past ca. 3000 years (Fig. 2 and Fig. 3; Table 1). Transverse dunes are mobile landforms and the OSL ages generated indicate periods of stabilization or transition out of the mobile phase. The lowest eolian unit is a silt-rich loess deposit overlying a well-developed paleosol with multiple argillic and carbonate horizons. The loess deposit comprises a massive, very well sorted medium silt deposit with no sand particles or bedding structures. A fine-quartz separate from this loess yielded an OSL age of 3145 ± 220 yr (1140 ± 220 BC, UIC1548). The overlying unit is a discontinuous, very well-sorted fine- to medium sand filling hollows on the paleolandscape and reflects sand sheet deposition with constraining ages between 1700 and 1525 yr (Table 1). The uppermost sedimentary unit includes mm-scale, inclined laminae of fine- to medium sand reflecting dune movement. OSL ages on quartz sand grains from the uppermost unit yielded ages of 1220 ± 80 yr (AD 785 ± 80, UIC1578), 825 ± 60 yr (AD 1180 ± 60, UIC1545) and 780 ± 50 yr (AD 1225 ± 50, UIC1577).

Figure 3. Northeast facing photograph of Trench T-1 (trowel handle = 12 cm; S. Forman photograph).

Trench T-2 was located 3.5 km northeast of the Gila River and a 13.5-m-long section was excavated in a stable transverse dune to a maximum depth of 1.5 m. This trench exposed massive, very well sorted fine to medium sands (Fig. 4). There was a 25-cm-thick soil developed that caps the transverse dune indicating a period of recent landform stability. Quartz grains from this dune deposit yielded OSL ages of 1885 ± 140 yr (AD 120 ± 140, UIC1549) and 1360 ± 110 yr (AD 645 ± 110, UIC1546).

Trench T-A was located within the archeological site GR-1442, <1 km north and east of the Gila River (Fig. 5). In a geomorphic assessment of the site, Waters (2005) records a 1.5- to 2-m-thick eolian mantle resting unconformably atop an eroded Pleistocene alluvial terrace (T-3) of the Gila River. The terrace deposits have soil with well-developed argillic and calcic horizons. Quartz grains from the base of this eolian sand yielded OSL ages 1990 ± 185 yr (AD 15 ± 185, UIC1759) and 1950 ± 150 yr (AD 55 ± 150, UIC1754).

Trench T-B was located within archeological site GR-893, adjacent to a small ephemeral wash and <1 km west of the Gila River. The landform on which Trench T-B is situated is informally called "Santa Cruz Island" because bifurcating forks of the Santa Cruz Wash surround this landform. A composite profile across the site shows the accretion of a well-sorted, culturally sterile eolian deposit interpreted as a transverse dune atop the T-2 terrace of the middle Gila River (Waters, 2005; Ravesloot et al., 2007). Six OSL ages ranging from ca. 690 to 315 yr (AD 1315 to 1690; Table 1) from eolian sand capping the site and ten calibrated AMS ^{14}C ages between ca. 1270 and 550 cal yr BP (AD 680 and 1400; Table 2) from subjacent archeological features, were generated from this site (Fig. 5 and Fig. 6). Additionally, ceramic sherds recovered from the archeological features were used to bracket the chronology.

Eolian depositional events

Eolian deposition is difficult to separate into precise, sequenced events with a distinct beginning and end because sediments move and settle on various temporal scales in intervals of days, months or years. It is not possible to constrain precisely the onset and termination of eolian activity from each analyzed profile: eolian strata are difficult to individually discriminate, it is impractical to date every stratum, and it is not feasible to obtain a reliable age on near-surface sediments. We present evidence for burial times of sediments based on the OSL and ^{14}C chronology from four trenches adjacent to the middle Gila River, but the duration and geographic extent of eolian activity in this area could have exceeded what our analysis covers. The results of our study correlate sediment movement to previously identified periods of Gila River aggradation and incision, as well as climatic events recorded in various proxy records from south-central Arizona.

The stratigraphy of the four trenches analyzed in this study, coupled with OSL ages, indicates that there were at least four episodes of eolian deposition in the past ca. 3000 yr. The oldest identified eolian event is a loess deposit in Trench T-1 that dates to ca. 3145 yr (Fig. 2). Given that the deposit averages only 10–20 cm thick and the fact that desert loess requires specific sediment supply and trapping mechanisms that are not

https://doi.org/10.1016/j.yqres.2011.04.008 Published online by Cambridge University Press

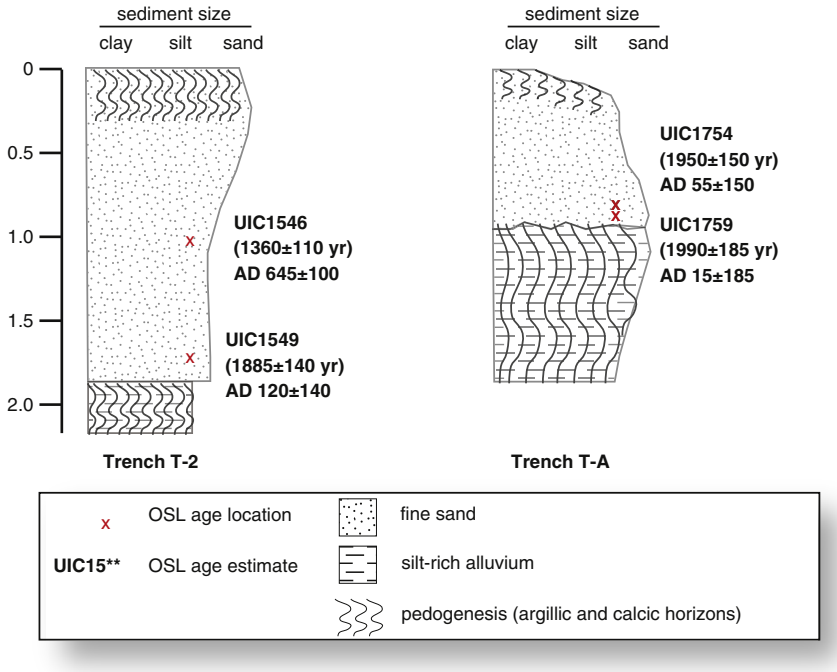

Figure 4. Stratigraphic profile of Trenches T-2 and T-A with locations of age assays.

likely to occur over long time periods (Tsoar and Pye, 1987), the OSL age from this stratigraphic unit is interpreted as the beginning and end of the deposit within the 1σ of statistical uncertainty. A period of eolian sand accumulation was initiated prior to ca. 1990 ± 185 yr (AD 15 ± 185) and six OSL proxies assayed from T-1, T-2 and T-A indicate variably distributed sand sheet formation or dune movement/accretion until at least 1360 ± 110 yr (AD 645 ± 110). A period of eolian deposition also occurred at ca. 800 yr (AD 1200), demarcated by dune movement at Trench T-1. Active sand-sheet deposition occurred at Trench T-B minimally from ca. 665 ± 50 yr to 315 ± 20 yr (AD 1340 to 1690).

Loess deposition at Trench T-1 at ca. 3145 yr (1140 BC) is likely derived from fine-grained overbank alluvial deposits, which were prevalent along the middle Gila River at that time (Waters and Ravesloot, 2000). In a study conducted adjacent to the lower Colorado River, increased ENSO periodicity dating from ca. 3200 to 2300 yr was linked to colluviation of upland sediments and deposition of alluvial fans (Bacon et al., 2010). Increases in rainfall typically witnessed in the American Southwest during the positive-phase (El Niño) ENSO dipole are counterbalanced by extreme droughts during the negative phase (Cayan et al., 1999). These climatic conditions produce a dynamic geomorphic setting in which loess deposition derived from eroded landforms or fluvial deposits is likely.

Trenches T-1, T-2 and T-A show initiation of eolian deposition ca. 1990 ± 185 yr, with continued accumulation of sand until at least 1360 ± 110 yr, and a younger event measured at ca. 800 yr (Fig. 7). The only potential source of eolian sand for these events is the adjacent Gila River. Water transport of sandy bedload can occur during the broadening of braided fluvial channels, which often transpires during storm events (Gomez, 1991; Bridge and Lunt, 2006). It is worth noting that Waters and Ravesloot (2000) record a period of enhanced overbank deposition ca. 2000 to 1000 cal yr BP on the Gila River floodplain, providing ample material for eolian entrainment. Increased flow variability within fluvial channels and storm-generated colluvium derived from sparsely vegetated landforms may also provide sediment supply for sand dunes (Lancaster, 1997; Clarke and Rendell, 1998; Hesse et al., 2004:96). In both cases, eolian activity reflects wind and sediment supply and is not necessarily a proxy for aridity. Aggradation along alluvial channel margins can, in fact, represent pluvial conditions (Lancaster and Tchakerian, 2003). The accretion of these sediments probably occurred episodically over decades to centuries.

Table 2
Radiocarbon assays on archeological features from GR-893 (Trench T-B).

Depositional context; Feature #	Material analyzed	Lab #	$^{13}C/^{14}C$ ratio	^{14}C age (^{14}C yr BP)	1σ cal age (cal yr BP)[a]	1σ cal age (yr AD)[a]
Midden fill; F3	Maize cupule	AA-69865	−9.7	1243 ± 45	1090–1270	680–860
Non-thermal pit fill; F17	Maize cupule	AA-69866	−11.3	1162 ± 49	1000–1180	770–950
Non-thermal pit fill; F46	Maize cupule	AA-69867	−10.2	621 ± 33	555–655	1295–1395
Non-thermal pit fill; F71	Maize cupule	AA-69868	−11.1	1163 ± 39	1000–1170	780–950
Thermal pit fill; F72	Maize cob	AA-69869	−10.0	641 ± 31	560–660	1290–1390
Non-thermal pit fill; F93	Maize cupule	AA-69871	−10.6	1059 ± 36	930–1050	900–1020
Thermal pit fill; F99	Maize cupule	AA-69872	−10.0	672 ± 32	560–680	1270–1390
Thermal pit fill; F112	Maize cupule	AA-69873	−9.9	665 ± 35	560–670	1280–1390
Thermal pit fill; F100	Maize cupule	AA-69874	−9.8	633 ± 31	560–660	1290–1390
Non-thermal pit fill; F114	Maize cupule	AA-69875	−10.6	1158 ± 32	1000–1170	780–950
Midden fill; F3	Maize cupule	AA-70566	−11.3	967 ± 32	800–930	1020–1150
Non-thermal pit fill; F46	Maize cupule	AA-70567	−10.5	654 ± 59	550–670	1280–1400

[a] Radiocarbon age calibration performed using OxCal v3.10 as reported in Woodson et al. (2007).

https://doi.org/10.1016/j.yqres.2011.04.008 Published online by Cambridge University Press

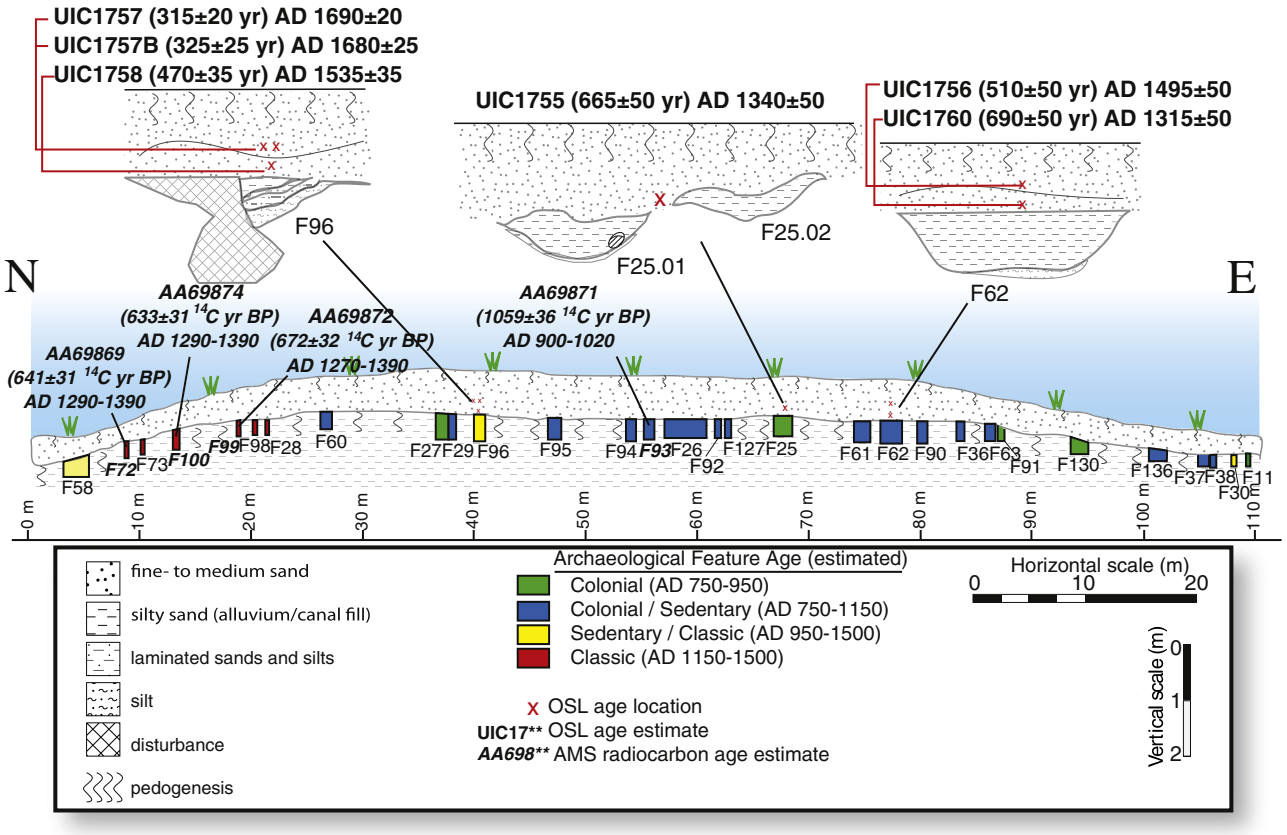

Figure 5. Stratigraphic profile for Trench T-B showing feature exposures, geomorphic interpretations, and chronometric ages.

Trench T-B (GR-893) exposes a sand-sheet deposit filling irrigation canals (Figs. 5–7, Event 4). The sediment supply for the sand sheet came either from easterly winds transporting Gila River alluvium or westerly winds transporting colluvium from the nearby Estrella Mountains. Based on the aggregate OSL and ^{14}C chronology, in addition to relative dating using ceramic sherds from archeological features, the landform appears to fill in from southeast to northwest. If so, then easterly winds were responsible for eolian deposition. Although sand sheet deposits were likely disruptive to the inhabitants of site GR-893, they do not necessarily reflect regional aridity in excess of previous conditions.

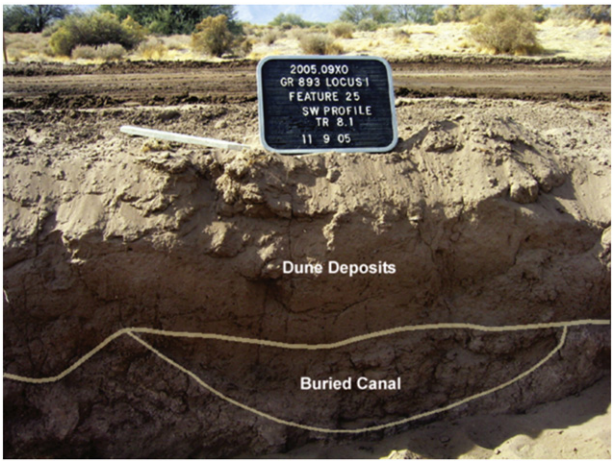

Fig. 6. Canal (Feature 25.01) buried under eolian deposits at GR-893.

Paleoenvironmental and demographic context of eolian activity

Regional aridity proxies and fluvial flow reconstructions indicate that late Holocene eolian activation events detected within the GRIC may relate to streamflow variability (Fig. 8). One measure of climatic conditions that drive this variability is the Palmer Drought Severity Index (PDSI), which was developed by William Palmer (1965) as a relative, standardized index of soil moisture that is calibrated regionally (Table 3). Reconstructed PDSI from the areas surrounding the GRIC (Ni et al., 2002b; Cook et al., 2004a; Graybill et al., 2006) show strongly negative values centered on AD 150, 300–500, 750, 1200–1250, and 1950. Positive PDSI values are recorded at AD 175–300, 1025–1100, 1300–1350, 1400–1450 (see also Ni et al., 2002a), and broadly from 1600 to 1950 with numerous exceptional negative years interspersed within the sequence. Likewise, reconstructed streamflows for the Salt and Gila Rivers (Graybill et al., 2006) show strong decadal-scale variability in hydrology with major pluviation events recorded ca. AD 1400, and from AD 1800–1950 (see also Ni et al., 2002a) in both basins and AD 750, 800, 1500 and 1750 within the Salt River catchment only (see also Palacios-Fest, 1997). Graybill et al. (2006) infer record-high streamflow volumes (2.88 million acre-feet/yr) in the Gila River catchment at AD 749, whereas Cook et al. (2004a,b) project PDSI values <−5 between AD 738 and 751, which is 2–3σ lower than the statistical mean (−1.46).

When all of the proxy records are compared to each other, three specific regionally arid events stand out, at ca. AD 1225, 1575, and 1950 (Ni et al., 2002b; Cook et al., 2004a; Graybill et al., 2006). These

https://doi.org/10.1016/j.yqres.2011.04.008 Published online by Cambridge University Press

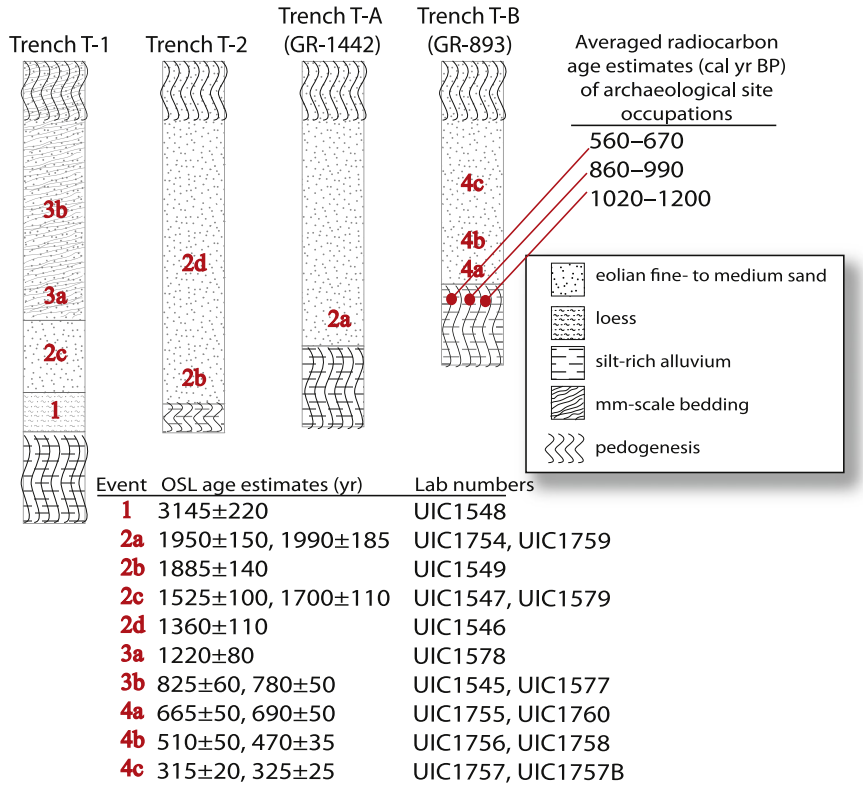

Figure 7. Representative profiles of the study location.

periods are especially noteworthy because the 10-year running averages are in general agreement that rainfall is significantly less than the statistical mean within the stream catchments of central and southern Arizona. Overall, the proxy data show oscillating wet–dry regimes within the Gila and Salt River catchments for the past 2000 years. Wet periods would have transported sediment in the streams, which would become mobilized by wind during the subsequent arid periods.

A number of severe droughts in the past millennium in the United States (Stahle et al., 2007) may have enhanced dune movement within the Gila River Basin. Of particular note is dune movement ca. 825–665 yr (AD 1180–1340), coincident with the Great Basin Drought (Benson et al., 2007) and shifting of the Hohokam population center from the middle Gila River toward the lower Salt River (Gregory, 1987; Bayman, 2001; Waters and Ravesloot, 2001; Ravesloot and Waters, 2002–2004). One of the phases of measured eolian activity in Trench T-B was identified as occurring ca. AD 1500, and coincides with the 16th century megadrought that impacted much of the western United States (Cook et al., 2007; Stahle et al., 2007). The lateral sequence of OSL ages at archeological site GR-893 decreases in age from 690 to 315 yr (AD 1315 to 1690) along a general east-to-west trajectory (Fig. 5). Eolian sediment accretion began concurrent to the later phases of GR-893 site occupation, forcing the inhabitants to move west away from the encroaching sand and persisted after its abandonment.

Our results suggest that the eolian sand depositional record for the Gila River is episodic (Fig. 7). There is an accumulation of eolian sand between 1990 ± 185 yr and 1700 ± 110 yr (ca. AD 200 ± 200) that is documented at Trenches T-1, T-2, and T-A. Eolian deposition continued in places until at least 1360 ± 110 yr (AD 650). Rapid dune migration is documented at Trench T-1 ca. 800 yr (AD 1200) based on preserved inclined bedding structures. Sand sheet deposition occurred in Trench T-B, infilling irrigation canals minimally between 690 and 315 yr (AD 1315–1690). It is difficult to implicate specific drought or pluvial periods in eolian deposition because of the variable spatial signature of eolian deposition and the apparent broad temporal occurrence of eolian events. A temporally sustained supply of sand may be associated with consistent sediment availability within the Gila River channel. Indeed, sand-sheet emplacement between the 14th and 18th centuries in Trench T-B may correspond to a period of channel narrowing/infilling with sediments followed by channel stability of the Gila River (Waters and Ravesloot, 2000), and generally more-pluvial-than-mean conditions (Palacios-Fest, 1997; Ni et al., 2002a,b; Cook et al., 2004a; Graybill et al., 2006). Ely (1997) reports high-magnitude flooding across the American Southwest >600 yr (AD 1400) related to accelerating periodicity of ENSO.

A dynamic fluvial and eolian system may reflect highly variable precipitation, possibly as a result of higher amplitude ENSO variability in the past ca. 2000 years (Moy et al., 2002; Lachniet et al., 2004; Woodhouse et al., 2005; Bacon et al., 2010). Winter precipitation within southern Arizona is generally greater during El-Niño phase oscillations, particularly when coupled with warm phase 25–35 yr cycles of PDO (Andrade and Sellers, 1988; Cayan et al., 1999; Goodrich, 2004; Wagner et al., 2010). This alternates with reduced precipitation across Arizona during the La Niña phase of the ENSO cycle and cold PDO phase (Cayan et al., 1999; Goodrich, 2004). High frequency between opposite phases of the pressure and temperature indexes result in close time-interval cycling of extreme weather phenomena in the American Southwest (Cayan et al., 1999). These conditions are favorable for high-volume fluvial sediment transport, channel braiding and point-bar accretion (Bookhagen et al., 2005; Moreno et al., 2008), which would present a ready-made sediment source for eolian entrainment.

Conversely, landform stability as indicated by soil development and intensive human habitation of archeological site GR-893 (Trench T-B) corresponds to three general time periods, which statistically overlap at 1σ. Aggregate mean radiocarbon age calculations from 12 assays indicate cultural activity on the landform ca. 1020–1200 cal yr BP (AD 750–930; AA69865; AA69866; AA69868; AA69875), ca. 860–990 cal yr BP (AD 960–1090; AA69871; AA70566) and ca. 560–

https://doi.org/10.1016/j.yqres.2011.04.008 Published online by Cambridge University Press

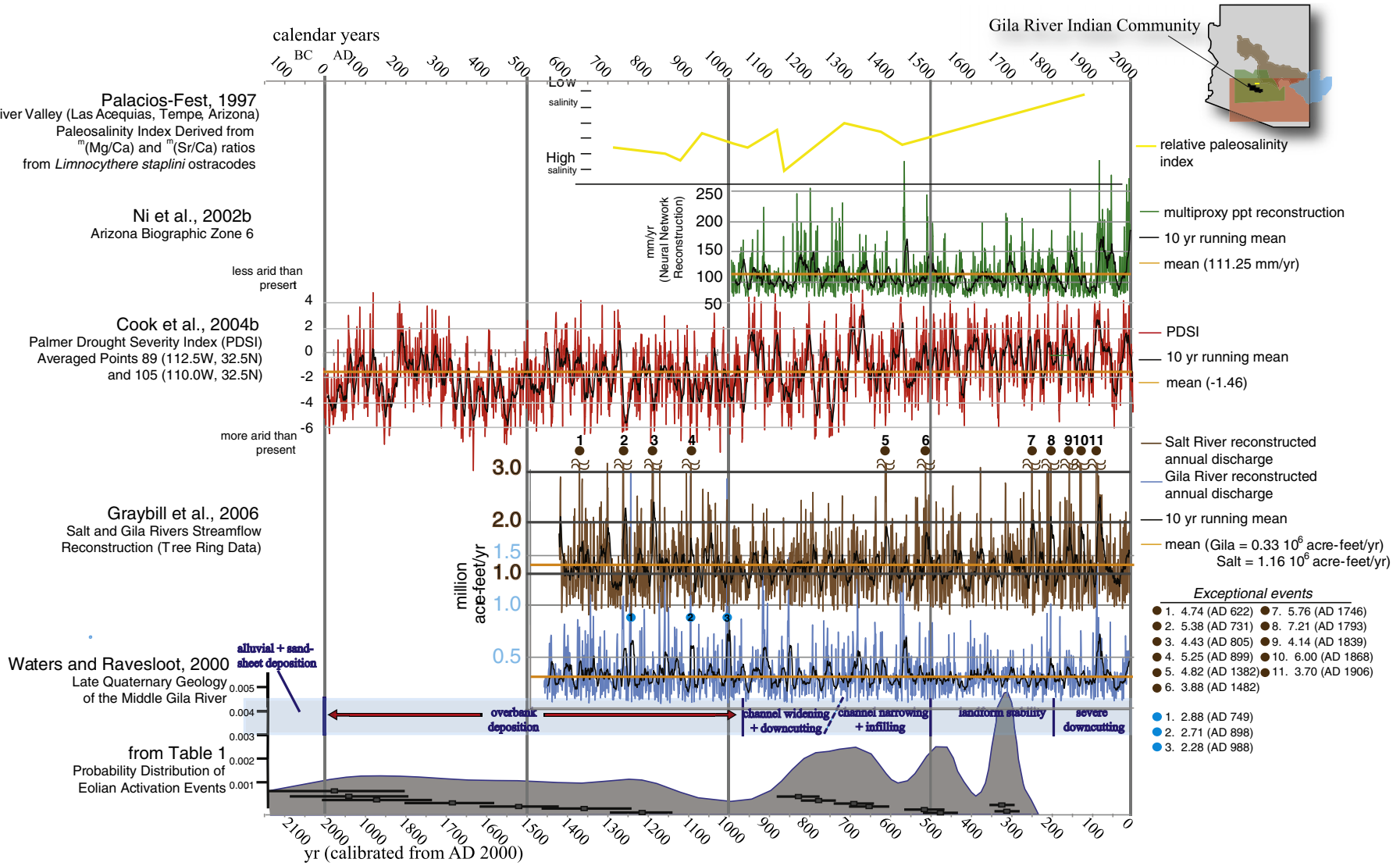

Figure 8. Comparative paleoclimatic reconstructions from southern Arizona and eolian activation events from the GRIC.

Table 3
PDSI values in relation to relative soil moisture conditions.

4.0 or more	Extremely wet
3.0 to 3.99	Very wet
2.0 to 2.99	Moderately wet
1.0 to 1.99	Slightly wet
0.5 to 0.99	Incipient wet spell
0.49 to −0.49	Near normal
−0.5 to −0.99	Incipient dry spell
−1.0 to −1.99	Mild drought
−2.0 to −2.99	Moderate drought
−3.0 to −3.99	Severe drought
−4.0 or less	Extreme drought

670 cal yr BP (AD 1280–1390; AA69867; AA69869; AA69872; AA69873; AA69874; AA70567). At archeological site GR-893 (Trench T-B), relative dating using ceramic sherds, radiocarbon, and OSL ages overlap statistically, which may indicate that initial sand sheet deposition and canal infilling began just prior to site abandonment (Woodson et al., 2007). Based on the features and eolian deposits identified, prehistoric humans shifted settlements laterally, westward to the leeside of the landform, possibly to avoid the encroaching sand. The primary eolian event as measured by canal infilling occurred at the southeastern end of the site and sand sheet deposition appears to have migrated laterally and aggraded to the northwest until ca. 315 yr (AD 1690). It is significant to note that canal irrigation was practiced through the duration of site occupation (Ravesloot et al., 2007), which may have contributed to soil development and certainly was instrumental in Hohokam resource buffering in an arid climate.

Geomorphic analysis of the sediment profiles indicates a period of landform stability in the historic period (>AD 1700) as reflected in Entisol soil development capping the dunes, which agrees with the dendroclimatological (Grissino-Mayer, 1996; Jain et al., 2002; Ni et al., 2002b; Cook et al., 2004a; Graybill et al., 2006; Stahle et al., 2007) and historic records (Jain et al., 2002; Committee on the Scientific Bases of Colorado River Basin Water Management, 2007) showing strong regional pluviation in the early 20th century. Fluvial incision of the Gila River within the historic period is also well established (Wilson, 1999; Waters and Ravesloot, 2000), which would have resulted in less overbank deposition of fine sands on the fluvial margins. Historic-period fluvial incision has been tied to diversion of upstream headwaters of the Gila River for Euroamerican agriculture (Waters and Ravesloot, 2001). Ultimately, landform stability and soil development capping eolian landforms tested in the present project can be seen as a result of more-pluvial-than-mean conditions (cf. Woodhouse et al., 2005) and anthropomorphic reduction in eolian sediment supply during the historic period.

Periods of heightened sand sheet deposition documented on the GRIC are probably associated with increased eolian sediment supply within the Gila River. Initial transverse dune formation and sand sheet deposition may correlate to periods of flow variability and/or overbank sedimentation of the Gila River floodplain. Burial of sediments and soil development corresponds to historic-era reduced sediment supply. Further OSL dating of eolian sequences is warranted to define better the spatial and temporal signature of dune reactivation and periods of sand sheet accretion, a very common surficial deposit at GRIC. In turn, a well-vetted chronology from the dune system, integrated with alluvial flood proxies of the Gila River (e.g., Waters and Ravesloot, 2001) and the chronology for canal construction and utilization will ultimately inform how the prehistoric inhabitants of the GRIC adapted to climate variability during the Holocene.

Conclusion

A nascent stratigraphic record and associated OSL ages on eolian sediment adjacent to the middle Gila River indicates four eolian depositional events at ca. 3145 ± 220 yr, 1950–1360 yr, 800 ± 100 yr, and 690–315 yr. The oldest eolian event is a 10–20 cm thick desert loess deposit dated to 3145 yr. The deposition of eolian sand in the past 2000 years is associated with flow variability of the Gila River, though eolian events that initiate at 800 and 500 yr (AD 1200 and 1500) are concordant with megadroughts in the southwestern United States (Cook et al., 2007; Stahle et al., 2007). This interpretation agrees broadly with geomorphic analyses of eolian deposition in the Mohave Desert (Lancaster and Tchakerian, 2003) of southern California, where sediment supply is the primary factor for dune formation and movement. In arid ecosystems such as the Sonoran and Mohave Deserts, vegetation is sparse, even during pluvial periods. Thus, precipitation and temperature variations have a secondary impact on eolian processes, compared to semi-arid grasslands, such as the Great Plains (cf. Wolfe et al., 2001) where such sediments are normally trapped by vegetation. The development of dune systems and associated sand sheet deposits adjacent to the Gila River reflect complex association between source, availability and regional aridity in the late Holocene.

Acknowledgments

This research was undertaken in conjunction with the Gila River Indian Community, Cultural Resource Management Program and the Pima–Maricopa Irrigation Project under funding from the Department of Interior, U.S. Bureau of Reclamation, under the Tribal Self-Governance Act (PL 103–413), for the design and development of a water delivery system utilizing Central Arizona Project water. Thanks to J. Andrew Darling, M. Kyle Woodson, and GRIC-CRMP staff who facilitated completion of this project. The cartographic skills of Lynn Simon, Russ Talas and Brian Lewis are especially recognized. The laboratory analytical skills of Jeaneth Gomez and James Pierson at the Luminescence Dating Research Laboratory at UIC were essential to completion of this project. Daniel Muhs and two anonymous reviewers greatly strengthened the quality of the manuscript, and we are very grateful for their insights.

References

Aitken, M.J., 1998. An Introduction to Optical Dating: The Dating of Quaternary Sediments by the Use of Photon-stimulated Luminescence. Oxford University Press, New York.
Anderson, R.S., Haff, P.K., 1988. Simulation of eolian saltation. Science 241, 820–823.
Anderson, R.S., Hallet, B., 1986. Sediment transport by wind: toward a general model. Geological Society of America Bulletin 97, 523–535.
Andrade Jr., E.R., Sellers, W.D., 1988. El Niño and its effect on precipitation in Arizona and western New Mexico. International Journal of Climatology 8, 403–410.
Bacon, S.N., McDonald, E.V., Caldwell, T.G., Dalldorf, G.K., 2010. Timing and distribution of allivial fan sedimentation in response to strengthening of Late Holocene ENSO variability in the Sonoran Desert, southwestern Arizona. Quaternary Research 73, 425–438.
Bagnold, R.A., 1941. The Physics of Blown Sand and Desert Dunes. Methuen & Co Ltd, London.
Bailey, S.D., Wintle, A.G., Duller, G.A.T., Bristow, C.S., 2001. Sand deposition during the last millennium at Aberffraw, Anglesey, North Wales as determined by OSL dating of quartz. Quaternary Science Reviews 20, 701–704.
Ballarini, M., Wallinga, J., Murray, A.S., van Heteren, S., Oost, A.P., Bos, A.J.J., van Ejik, C. W.E., 2003. Optical dating of young coastal dunes on a decadal time scale. Quaternary Science Reviews 22, 1011–1017.
Bayman, J.M., 2001. The Hohokam of southwest North America. Journal of World Prehistory 15, 257–311.
Benson, L., Petersen, K., Stein, J., 2007. Anasazi (pre-Columbian Native-American) migrations during the middle-12th and late-13th centuries — were they drought induced? Climatic Change 83, 187–213.
Bettis, E.A., Muhs, D.R., Roberts, H.M., Wintle, A.G., 2003. Last glacial loess in the conterminous USA. Quaternary Science Reviews 22, 1907–1946.
Biondi, F., Gershunov, A., Cayan, D.R., 2001. North Pacific decadal climate variability since 1661. Journal of Climate 14, 5–10.
Bookhagen, B., Thiede, R.C., Strecker, M.R., 2005. Abnormal monsoon years and their control on erosion and sediment flux in the high, arid northwest Himalaya. Earth and Planetary Science Letters 231, 131–146.
Bøtter-Jensen, L., Bulur, E., Duller, G.A.T., Murray, A.S., 2000. Advances in luminescence instrument systems. Radiation Measurements 32, 523–528.
Bridge, J.S., Lunt, I.A., 2006. Depositional models of braided rivers. In: Sambrook Smith, G. H., Best, J.L., Bristow, C.S., Petts, G.E. (Eds.), Braided Rivers: Process, Deposits, Ecology and Management. Blackwell Publishing, Malden, Massachusetts, pp. 11–50.

https://doi.org/10.1016/j.yqres.2011.04.008 Published online by Cambridge University Press

Butterfield, G.R., 1998. Transitional behaviour of saltation: wind tunnel observations of unsteady winds. Journal of Arid Environments 39, 377–394.
Camp, P., 1986. Soil survey of the Gila River Indian Reservation, Arizona, parts of Maricopa and Pinal Counties. Manuscript on file at the Soil Conservation Service, Chandler, Arizona.
Cayan, D.R., Redmond, K.T., Riddle, L.G., 1999. ENSO and hydrologic extremes in the western United States. Journal of Climate 12, 2881–2893.
Clarke, M.L., Rendell, H.M., 1998. Climate change impacts on sand supply and the formation of desert sand dunes in the South-West U.S.A. Journal of Arid Environments 39, 517–531.
Clemmensen, L.B., Murray, A.S., 2006. The termination of the last major phase of aeolian sand movement, coastal dunefields, Denmark. Earth Surface Processes and Landforms 31, 795–808.
Committee on the Scientific Bases of Colorado River Basin Water Management, 2007. Colorado River Basin Water Management: Evaluating and Adjusting to Hydroclimatic Variability. The National Academies Press, Washington, D.C.
Cook, E.R., Woodhouse, C.A., Eakin, C.M., Meko, D.M., Stahle, D.W., 2004a. Long-term aridity changes in the western United States. Science 306, 1015–1018.
Cook, E.R., Woodhouse, C.A., Eakin, C.M., Meko, D.M., Stahle, D.W., 2004b. North American summer PDSI reconstructions. IGBP pages/World Data Center for Paleoclimatology Data Contribution Series # 2004–045. NOAA/NGDC Paleoclimatology Program, Boulder, Colorado.
Cook, E.R., Seager, R., Cane, M.A., Stahle, D.W., 2007. North American drought: reconstructions, causes, and consequences. Earth Science Reviews 81, 93–134.
Darling, J.A., Ravesloot, J.C., Waters, M.R., 2004. Village drift and riverine settlement: modeling Akimel O'odham land use. American Anthropologist 106, 282–295.
Duller, G.A.T., Bøtter-Jensen, L., Murray, A.S., 2003. Combining infrared and green-laser stimulation sources in single-grain luminescence measurements of feldspar and quartz. Radiation Measurements 37, 543–550.
Eiselt, J.S., Woodson, M.K., Touchin, J., Davis, E., 2002. A cultural resources assessment of the Casa Blanca Management Area, Pima–Maricopa Irrigation Project (P-MIP), Gila River Indian Community, Arizona. P-MIP Report No. 8. Cultural Resource Management Program, Gila River Indian Community, Sacaton, Arizona.
Ely, L.L., 1997. Response of extreme floods in the southwestern United States to climatic variations in the Late Holocene. Geomorphology 19, 175–201.
Fain, J., Soumana, S., Montret, M., Miallier, D., Pilleyre, T., Sanzelle, S., 1999. Luminescence and ESR dating-beta-dose attenuation for various grain shapes calculated by a Monte-Carlo method. Quaternary Science Reviews 18, 231–234.
Fearnehough, W., Fullen, M.A., Mitchell, D.J., Trueman, I.C., Zhang, J., 1998. Aeolian deposition and its effect on soil and vegetation changes on stabilised desert dunes in northern China. Geomorphology 23, 171–182.
Fish, S.K., Fish, P.R., 2008. The Hohokam Millennium. School for Advanced Research Press, Santa Fe, New Mexico.
Forman, S.L., Pierson, J., 2003. Formation of linear and parabolic dunes on the eastern Snake River plain, Idaho in the nineteenth century. Geomorphology 56, 189–200.
Forman, S.L., Spaeth, M., Marín, L., Pierson, J., Gomez, J., Bunch, F., Valdez, A., 2006. Episodic Late Holocene dune movements on the sand-sheet area, Great Sand Dunes National Park and Preserve, San Luis Valley, Colorado, USA. Quaternary Research 66, 97–108.
Galbraith, R.F., Roberts, R.G., Laslett, G.M., Yoshida, H., Olley, J.M., 1999. Optical dating of single and multiple grains of quartz from Jinmium Rock Shelter, northern Australia: part I, experimental design and statistical models. Archaeometry 41, 339–364.
Gomez, B., 1991. Bedload transport. Earth Science Reviews 31, 89–132.
Goodrich, G.B., 2004. Modulation of the winter ENSO Arizona climate signal by the Pacific Decadal Oscillation. Journal of the Arizona–Nevada Academy of Science 36, 88–94.
Goossens, D., Offer, Z.Y., 1997. Aeolian dust erosion on different types of hills in a rocky desert: wind tunnel simulations and field measurements. Journal of Arid Environments 37, 209–229.
Graybill, D.A., Gregory, D.A., Funkhouser, G.S., Nials, F., 2006. Long-term streamflow reconstructions, river channel morphology, and aboriginal irrigation systems along the Salt and Gila Rivers. In: Doyel, D.E., Dean, J.S. (Eds.), Environmental Change and Human Adaptation in the Ancient American Southwest. University of Utah Press, Salt Lake City, pp. 69–123.
Gregory, D.A., 1987. The morphology of platform mounds and the structure of Classic Period Hohokam sites. In: Doyel, D.E. (Ed.), The Hohokam Village: Site Organization and Structure. Southwestern and Rocky Mountain Division, American Association for the Advancement of Science, Glenwood Springs, Colorado, pp. 183–210.
Grissino-Mayer, H.D., 1996. A 2129-year reconstruction of precipitation for northwestern New Mexico, USA. In: Dean, J.S., Meko, D.M., Swetnam, T.W. (Eds.), Tree Rings, Environment and Humanity: Proceedings of the International Conference, Tucson, AZ, May 17–21, 1994. Radiocarbon, Tucson, Arizona, pp. 191–204.
Haury, E.W., 1976. The Hohokam: Desert Farmers and Craftsmen: Excavations at Snaketown, 1964–1965. University of Arizona Press, Tucson.
Herweijer, C., Seager, R., Cook, E.R., Emile-Geay, J., 2007. North American droughts of the last millenium from a gridded network of tree-ring data. Journal of Climate 20, 1353–1376.
Hesse, P.P., Magee, J.W., van der Kaars, S., 2004. Late Quaternary climates of the Australian arid zone: a review. Quaternary International 118–119, 87–102.
Hirschboek, K., 1985. Hydroclimatology of Flow Events in the Gila River Basin, Central and Southern Arizona. Department of Geosciences, University of Arizona, Tucson.
Huckleberry, G.A., 1993. Late-Holocene Stream Dynamics on the Middle Gila River, Pinal County, Arizona. Department of Geosciences, University of Arizona, Tucson.
Huckleberry, G.A., 1994. Surficial Geology of the Santan Mountains Piedmont Area, Northern Pinal and Eastern Maricopa County Area, Arizona. Arizona Geological Survey, Tucson.
Huckleberry, G.A., 1995. Archaeological implications of Late Holocene channel changes on the middle Gila River, Arizona. Geoarchaeology 10, 159–182.
Jain, S., Woodhouse, C.A., Hoerling, M.P., 2002. Multidecadal streamflow regimes in the interior western United States: implications for the vulnerability of water resources. Geophysical Research Letters 29, 2036. doi:10.1029/2001GL014278.
Kocurek, G., Lancaster, N., 1999. Aeolian system sediment state: theory and Mojave Desert Kelso dune field example. Sedimentology 46, 505–515.
Kohfeld, K.E., Harrison, S.P., 2003. Glacial–interglacial changes in dust deposition on the Chinese loess plateau. Quaternary Science Reviews 22, 1859–1878.
Lachniet, M.S., Burns, S.J., Piperno, D.R., Asmerom, Y., Polyak, V.J., Moy, C.M., Christenson, K., 2004. A 1500-year El Niño/Southern Oscillation and rainfall history for the Isthmus of Panama from speleothem calcite. Journal of Geophysical Research, Atmospheres 109, D20117.
Lancaster, N., 1997. Response of eolian geomorphic systems to minor climate change: examples from the southern Californian deserts. Geomorphology 19, 333–347.
Lancaster, N., Tchakerian, V.P., 2003. Late Quaternary eolian dynamics. In: Enzell, Y., Wells, S.G., Lancaster, N. (Eds.), Paleoenvironments and Paleogydrology of the Mohave and Southern Great Basin Deserts, Boulder, Colorado. Special Paper No. 368. Geological Society of America, Boulder, Colorado, pp. 231–249.
Mejdahl, V., Christiansen, H.H., 1994. Procedures used for luminescence dating of sediments. Boreas 13, 403–406.
Moreno, A., Valero-Garcés, B.L., González-Sampériz, P., Rico, M., 2008. Flood response to rainfall variability during the last 2000 years inferred from the Taravilla Lake record (central Iberian range, Spain). Journal of Paleolimnology 40, 943–961.
Moy, C.M., Seltzer, G.O., Rodbell, D.T., Anderson, D.M., 2002. Variability of El Niño/Southern Oscillation activity at millennial timescales during the Holocene Epoch. Nature 420, 162–165.
Muhs, D.R., Bettis, E.A., 2003. Quaternary loess–paleosol sequences as examples of climate driven-sedimentary extremes. In: Chan, M.A., Archer, A.W. (Eds.), Extreme Depositional Environments: Mega End Members in Geologic Time: Geological Society of America Special Paper, 370, pp. 53–74. Boulder, Colorado.
Muhs, D.R., Reynolds, R.L., Been, J., Skipp, G., 2003. Eolian sand transport pathways in the southwestern United States: importance of the Colorado River and local sources. Quaternary International 104, 3–18.
Murray, A.S., Clemmensen, L.B., 2001. Luminescence dating of Holocene aeolian sand movement, Thy, Denmark. Quaternary Science Reviews 20, 751–754.
Murray, A.S., Wintle, A.G., 2003. The single aliquot regenerative dose protocol: potential for improvements in reliability. Radiation Measurements 37, 377–381.
National Climatic Data Center, 1998. Climatic and Wind Data for the United States. Online resource accessed July 6, 2010. http://www.ncdc.noaa.gov/oa/mpp/wind1996.pdf. National Oceanic and Atmospheric Administration, Asheville, North Carolina.
Ni, F., Cavazos, T., Hughes, M.K., Comrie, A.C., Funkhouser, G., 2002a. Cool-season precipitation in the southwestern USA since AD 1000: comparison of linear and nonlinear techniques for reconstruction. International Journal of Climatology 22, 1645–1662.
Ni, F., Cavazos, T., Hughes, M.K., Comrie, A.C., Funkhouser, G., 2002b. Southwestern USA linear regression and neural network precipitation reconstructions. International Tree-Ring Data Bank. IGBP pages/World Data Center for Paleoclimatology Data contribution series #2002-080. NOAA/NGDC Paleoclimatology Program, Boulder, Colorado.
Palacios-Fest, M.R., 1997. Paleoenvironmental reconstruction of human activity in Central Arizona using shell chemistry of Hohokam canal ostracodes. Geoarchaeology 12, 211–226.
Palmer, W.C., 1965. Meteorological drought. Research paper no. 45. Office of Climatology, U.S. Weather Bureau, U.S. Department of Commerce, Washington, D.C.
Porter, S.C., 2001. Chinese loess record of monsoon climate during the last glacial–interglacial cycle. Earth-Science Reviews 54, 115–128.
Prescott, J.R., Hutton, J.T., 1994. Cosmic ray contributions to dose rates for luminescence and ESR dating: large depths and long-term time variations. Radiation Measurements 23, 497–500.
Pye, K., 1995. The nature, origin and accumulation of loess. Quaternary Science Reviews 14, 653–667.
Pye, K., Tsoar, H., 1990. Aeolian Sand and Sand Dunes. Unwin Hyman, Boston.
Ravesloot, J.C., Waters, M.R., 2002–2004. Geoarchaeology and archaeological site patterning on the middle Gila River, Arizona. Journal of Field Archaeology 29, 203–214.
Ravesloot, J.C., Woodson, M.K., Boley, M.J., 2007. Results of testing and data recovery, SFPP, LP, East Line Expansion Project, Arizona portion. Cochise, Pima, Pinal, and Maricopa Counties, Arizona. WAS Technical Report No. 2007–04. William Self Associates, Inc, Tucson, Arizona.
Ravesloot, J.C., Darling, J.A., Waters, M.R., 2009. Hohokam and Pima–Maricopa irrigation agriculturalists. In: Fisher, C.T., Hill, J.B., Feinman, G.M. (Eds.), The Archaeology of Environmental Change: Socionatural Legacies of Degradation and Resilience. University of Arizona Press, Tucson, pp. 232–245.
Reheis, M.C., Reynolds, R.L., Goldstein, H., Roberts, H.M., Yount, J.C., Axford, Y., Cummings, L.S., Shearin, N., 2005. Late Quaternary eolian and alluvial response to paleoclimate, Canyonlands, southeastern Utah. Geological Society of America Bulletin 117, 1051–1069.
Sarre, R.D., 1987. Aeolian sand transport. Progress in Physical Geography 11, 157–182.
Sellars, W., Hill, R.H., 1974. Arizona Climate. University of Arizona Press, Tucson.
Shao, Y., 2000. Physics and Modeling of Wind Erosion. Kluwer Academic Publishers, Dordrecht.
Sheppard, P.R., Comrie, A.C., Packin, G.D., Angersbach, K., Hughes, M.K., 2002. The climate of the US Southwest. Climate Research 21, 219–238.
Singhvi, A.K., Bluszcz, A., Bateman, M.D., Rao, M.S., 2001. Luminescence dating of loess–palaeosol sequences and coversands: methodological aspects and palaeoclimatic implications. Earth Science Reviews 54, 193–211.

Smalley, I.J., 1966. The properties of glacial loess and the formation of loess deposits. Journal of Sedimentary Research 36, 669–676.
Smalley, I., 1995. Making the material: the formation of silt sized primary mineral particles for loess deposits. Quaternary Science Reviews 14, 645–651.
Smalley, I.J., Vita-Finzi, C., 1968. The formation of fine particles in sandy deserts and the nature of 'desert' loess. Journal of Sedimentary Research 38, 766–774.
Smith, W., 1986. The effects of eastern North Pacific tropical cyclones on the southwestern United States. N.O.A.A. Technical Memorandum NWS WR-197. U.S. Department of Commerce, Washington, D.C.
Stahle, D.W., Fye, F.K., Cook, E.R., Griffin, R.D., 2007. Tree-ring reconstructed megadroughts over North America since AD 1300. Climatic Change 83, 133–149.
Stokes, S., Bailey, R.M., Fedoroff, N., O'Marah, K.E., 2004. Optical dating of aeolian dynamism on the West African Sahelian margin. Geomorphology 59, 281–291.
Tchakerian, V.P., Lancaster, N., 2002. Late Quaternary arid/humid cycles in the Mojave Desert and western Great Basin of North America. Quaternary Science Reviews 21, 799–810.
Tsoar, H., Pye, K., 1987. Dust transport and the question of desert loess formation. Sedimentology 34, 139–153.
Wagner, J.D.M., Cole, J.E., Beck, J.W., Patchett, P.J., Henderson, G.M., Barnett, H.R., 2010. Moisture variability in the southwestern United States linked to abrupt glacial climate change. Nature Geoscience 10.1038/NGEO1707.
Waters, M.R., 1996. Surficial geologic map of the Gila River Indian Community. P-MIP Technical Report No. 96-1. Cultural Resource Management Program, Gila River Indian Community, Sacaton, Arizona.
Waters, M.R., 1998. The effect of landscape and hydrologic variables on the prehistoric Salado: Geoarchaeological investigations in the Tonto Basin, Arizona. Geoarchaeology 13, 105–160.
Waters, M.R., 2005. Geoarchaeological reconnaissance and evaluation of the East Line Expansion Project, Gila River Indian Reservation, Arizona. In: WIlliam Self Associates, ASU Office of Cultural Resource Management, Gila River Indian Community Cultural Resource Management Program (Eds.), Final Treatment Plan for Cultural Resources, SFPP East Line Expansion Project, Arizona Portion. William Self Associates, Inc, Tucson, Arizona.
Waters, M.R., 2008. Alluvial chronologies and archaeology of the Gila River drainage basin, Arizona. Geomorphology 101, 332–341.
Waters, M.R., Ravesloot, J.C., 2000. Late Quaternary geology of the middle Gila River, Gila River Indian Reservation, Arizona. Quaternary Research 54, 49–57.
Waters, M.R., Ravesloot, J.C., 2001. Landscape change and the cultural evolution of the Hohokam along the middle Gila River and other river valleys in South-Central Arizona. American Antiquity 66, 285–299.
Waters, M.R., Ravesloot, J.C., 2003. Disaster or catastrophe: human adaptation to high- and low-frequency landscape processes — a reply to Ensor, Ensor, and DeVries. American Antiquity 68, 400–405.
Williams, J.J., Butterfield, G.R., Clark, D.G., 1993. Aerodynamic entrainment threshold: effects of boundary layer flow conditions. Sedimentology 41, 309–328.
Wilson, J.P., 1999. Peoples of the middle Gila: A documentary history of the Pimas and Maricopas, 1500s-1945. Unpublished ms. on file, Cultural Resource Management Program, Gila River Indian Community, Sacaton, Arizona.
Wintle, A.G., Murray, A.S., 2006. A review of quartz Optically Stimulated Luminescence characteristics and their relevance in Single-Aliquot Regeneration dating protocols. Radiation Measurements 41, 369–391.
Wolfe, S.A., Huntley, D.J., David, P.P., Ollerhead, J., Sauchyn, D.J., MacDonald, G.M., 2001. Late 18th century drought-induced sand dune activity, Great Sand Hills, Saskatchewan. Canadian Journal of Earth Sciences 38, 105–117.
Woodhouse, C.A., Lukas, J.J., Brown, P.M., 2002. Drought in the western Great Plains, 1845–56 — impacts and implications. Bulletin of the American Meteorological Society 83, 1485–1493.
Woodhouse, C.A., Kunkel, K.E., Easterling, D.R., Cook, E.R., 2005. The twentieth-century pluvial in the western United States. Geophysical Research Letters 32, L07701.
Woodson, M.K., Ravesloot, J.C., Boley, M.J., Forman, S.L., 2007. Chronology. In: Ravesloot, J.C., Woodson, M.K., Boley, M.J. (Eds.), Testing and Data Recovery, SFPP, LP, East Line Expansion Project, Arizona portion: Cochise, Pima, Pinal, and Maricopa counties. WSA Technical Report No. 2007-04. William Self Associates, Inc, Tucson, Arizona, pp. 10.11–10.29.
Wright, J.S., 2001. "Desert" loess versus "glacial" loess: quartz silt formation, source areas and sediment pathways in the formation of loess deposits. Geomorphology 36, 231–256.
Wright, D.K., Forman, S.L., 2010. Geomorphological testing of eolian landforms, Gila River Indian Community, Arizona. P-MIP Tec Report 2008-05. Cultural Resource Management Program, Gila River Indian Community, Sacaton, Arizona.